Inorg. Chem. **1997,** *36,* 4789−4797

Reactivity of the Acyclic Diazadioxa Redox Active Ligand $[(C_5H_5)Fe(C_5H_4CH_2N(CH_3)(CH_2)_2OCH_2-)]_2$: NMR, Electrochemical, and Mössbauer Studies. Crystal Structure of Its Copper Complex

Béatrice Delavaux-Nicot,* Agnès Bigeard, Azzedine Bousseksou, Bruno Donnadieu, and Gérard Commenges

Laboratoire de Chimie de Coordination du CNRS, UPR 8241 liée par conventions à l'Université Paul
Sabatier et à l'Institut National Polytechnique de Toulouse, 205 route de Narbonne, 31077,
Toulouse Cedex 4, France

Received January 8, 1997[⊗]

Several novel diazadioxa ferrocenyl derivatives have been prepared along with their previously unknown electroactive precursor $[(C_5H_5)Fe(C_5H_4CH_2N(CH_3)(CH_2)_2OCH_2-)]_2$ (**2**). Di-N,N′-protonated and -methylated species $[\mathbf{2}(H)_2][X]_2$ (**3a**−**c**) (X = CF_3SO_3, BF_4, PF_6) and $[\mathbf{2}(Me)_2][CF_3SO_3]_2$ (**5**), and N−H−N monoprotonated species $[\mathbf{2}H][X]$ (**4a**−**c**) have been isolated in high yield. The efficient syntheses of compounds $[\mathbf{2}Na][PF_6]$ (**6**), $[\mathbf{2}Cu][CF_3SO_3]$ (**7**), $[\mathbf{2}Ag][CF_3SO_3]$ (**8**), and $[\mathbf{2}MCl_2]$ (M = Zn, Hg) (**9**, **10**) are reported. The crystal structure of complex **7** has been determined by X-ray analysis at 180 K. Crystal data: monoclinic $P2_1/c$, with $a = 11.511(2)$ Å, $b = 19.613(2)$ Å, $c = 14.493(2)$ Å, $\beta = 88.32(2)°$, $V = 3273.2(1)$ Å^3, $Z = 4$; $R = 0.034$, $R_w = 0.039$ for 3379 observations and 407 variable parameters. The copper(I) atom, bound to the two O and two N atoms of the ferrocenyl ligand, is in a very distorted tetrahedral geometry with a large N(1)CuN(2) angle (163.1(2)°). In cyclic voltammetry, **4a**−**c** undergo two quasi-reversible (Fe(II)/Fe(III)) redox processes at 0.1 V s^{-1}. Electrochemical studies of **3a**−**c**, **5**, **7**, and **8** show that diprotonation and dialkylation of **2** or complexation of a Cu (Ag) salt induces an anodic shift ranging from 240 to 110 mV. Chemical oxidation of **2** (5 equiv of Ag(I)) produces the cation $[\mathbf{2}(H)_2]^{4+}$ (**11**). The quantitative two-step electrochemical oxidation of **2** at controlled potential in CH_3CN also leads to **11**: an ECE mechanism, in which the diprotonated species plays a key role, is proposed. Mössbauer data of **2**, **3c**, **6**, **7**, **8**, and **11** are also presented.

Introduction

The design of receptors containing ferrocenyl groups for electrochemical recognition is a recurrent theme in contemporary chemistry.[1,2] One of our goals in this regard has been to synthesize new 1,2-disubstituted ferrocenyl compounds containing both a $(Ph)P(S)(NMeN{=}CH-)_2$ and a $(-CH_2NMe(CH_2)_2OCH_2-)_2$ moiety. Recently, we have shown that it is possible to selectively synthesize acyclic phosphorus-containing ferrocenyl ligands $Ph_{3-n}PX(NMeN{=}CHC_5H_4FeCp)_n$ (X = O, S; n = 2, 3), in high yield. These ligands show a remarkable ability to yield electroactive complexes with a copper(I) salt and $ZnCl_2$.[3] Our preliminary results have provided us with the opportunity to synthesize the new diferrocenyl compound $[(C_5H_5)Fe(C_5H_4CH_2N(CH_3)(CH_2)_2OCH_2-)]_2$ (**2**).[4] The most interesting feature of **2** is the combination of an electrochemically active ferrocene and a simple organic ether chain within the same molecule. In the neutral form, the diferrocene can bind a cation through its nitrogen and (or) oxygen donor sites; upon oxidation to ferrocenium, however, the unfavorable interaction of two cations in close proximity can lead to a destabilization of the complex, as shown for $PhPS(NMeN{=}CHC_5H_4FeCp)_2$ (**1**), and can provide an opportunity to recover both the ligand and cation. Except for crown ether chemistry, few studies of ether−cation complexation have been undertaken because ether−cation interactions are weak and therefore difficult to assess.[5]

In order to better understand the complexing and redox properties of the novel dimetallic complex **2** we decided to study its reactivity and to examine the electrochemical behavior of this ligand and of its new cationic derivatives. The synthesis and characterization of complexes obtained through protonation and methylation reactions of **2** are described in this paper. The electrochemical behavior of these compounds has allowed us to suggest a mechanism for the electrochemical oxidation of complex **2** in CH_3CN. The complexation reactions of **2** with Na(I), Cu(I), Ag(I), Zn(II), and Hg(II) compounds are reported, and the X-ray structure of the heterotrimetallic iron−copper complex $[\mathbf{2}Cu][CF_3SO_3]$ is presented.

Results and Discussion

1. Protonation and Methylation Reactions of Compound 2. Organic crown ethers and cryptands containing several diazaoxa chains are known to be easily protonated, and some of them may be used as pH sensors.[6] Recently, Plenio et al., in order to better understand the influence of the hardness

---

[⊗] Abstract published in *Advance ACS Abstracts*, August 15, 1997.

(1) See, for example: (a) Beer, P. D. *Chem. Soc. Rev.* **1989**, *18*, 409. (b) Beer, P. D. *Adv. Inorg. Chem.* **1992**, *39*, 79. (c) Constable, E. C. *Angew. Chem., Int. Ed. Engl.* **1991**, *30*, 407 and references therein. (d) Grossel, M. C.; Goldspink, M. R.; Hriljac, J. A.; Weston, S. C. *Organometallics* **1991**, *10*, 851 and references therein. (e) Medina, J. C.; Goodnow, T. T.; Rojas M. T.; Atwood, J. L.; Lynn, B. C.; Kaifer, A. E.; Gokel, G. W. *J. Am. Chem. Soc.* **1992**, *114*, 10583.

(2) Delavaux-Nicot, B.; Guari, Y.; Douziech, B.; Mathieu, R. *J. Chem. Soc., Chem. Commun.* **1995**, 585.

(3) (a) Delavaux-Nicot, B.; Lugan, N.; Mathieu, R.; Majoral, J.-P. *Inorg. Chem.* **1992**, *31*, 334. (b) Delavaux-Nicot, B.; Mathieu, R. *Phosphorus, Sulfur. Silicon Relat. Elem.* **1993**, *77*, 323. (c) Delavaux-Nicot, B.; Mathieu, R.; de Montauzon D.; Lavigne, G.; Majoral, J.-P. *Inorg. Chem.* **1994**, *33*, 334. (d) Delavaux-Nicot, B.; Douziech, B.; Mathieu, R.; Lavigne, G. *Inorg. Chem.* **1995**, *34*, 4256.

(4) Delavaux-Nicot, B.; Guari, Y.; Mathieu, R. *J. Organomet. Chem.* **1995**, *489*, C87.

(5) Wang, K.; Han, X.; Gross, R. W.; Gokel, G. W. *J. Am. Chem. Soc.* **1995**, *117*, 7680.

(6) Gokel, G. W. In *Crown Ethers and Cryptands*; Stoddart, J. F., Ed.; Royal Society of Chemistry: Cambridge, U.K., 1991; Chapter 5, 145 and references therein.

S0020-1669(97)00017-7 CCC: $14.00

Scheme 1

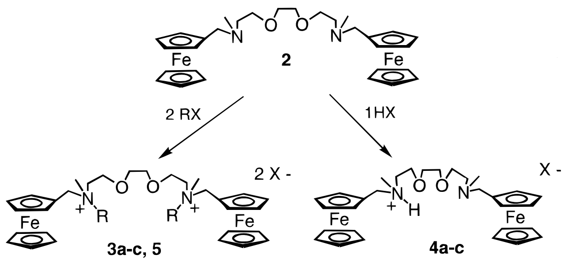

3a: R = H, X = CF_3SO_3,
3b: R = H, X = BF_4,
3c: R = H, X = PF_6
5: R = CH_3, X = CF_3SO_3,

4a, X = CF_3SO_3,
4b, X = BF_4,
4c, X = PF_6 ,(NH_4PF_6)

(charge-to-radius ratio) of a complexed cation on the electrochemistry of several ferrocene crowns and aza cryptands, investigated the effect of the hardest possible cation, H^+, on these systems.[7] In the case of compound **2**, the reaction with H^+ was particularly interesting since the stable diprotonated species seemed to play a key role in the electrochemical oxidation process of this starting complex (vide infra).

The one-pot synthesis of compound **2** was realized by reacting $[(C_5H_5)Fe(C_5H_4CH_2NMe_3)][I]$ with 0.5 equiv of 1,8-bis(methylamino)-3,6-dioxaoctane in water.[4] **2** reacts with 2 equiv of HX (X = CF_3SO_3, BF_4) to afford, after purification, $[\mathbf{2}(H)_2][X]_2$ (X = CF_3SO_3 (**3a**) and X = BF_4 (**3b**), in high yield (95–97%) as oils (Scheme 1). The structure of these molecules has been deduced from spectroscopic data. In particular, the protonation reaction has been confirmed by the appearence of a new signal at $\delta \approx 7$ ppm (^1H NMR, CD_3CN) attributed to the protons of the NH^+ groups.[8] 2D NMR experiments have been carried out for compound **2** and for the diprotonated complex **3a** and clearly verify the assignments. Elemental analyses and mass spectra are also in agreement with the proposed formulation (See Experimental Section).

Addition of NH_4PF_6 to a solution of compound **2** could lead to the new adduct $[\mathbf{2}NH_4][PF_6]$ with N^+H- - -N and N^+H- - -O (salt/ligand) interactions.[9] Attempts to crystallize this species from mixtures of NH_4PF_6 and **2**, in 1:1 and 1:2 stoichiometry in CH_3CN, according to established procedures,[9a] were unsuccessful.[10] However, when complex **2** was reacted with 2 equiv of NH_4PF_6, the product isolated after treatment was the diprotonated species $[\mathbf{2}(H)_2][PF_6]_2$ (**3c**). In contrast to **3a**,**b**, the product was obtained as a powder, and in the solid state, the ν (N^+H) (KBr) absorptions could be clearly located at 3199 cm^{-1}.[11]

Reaction of compound **2** with HCF_3SO_3, $HBF_4{\cdot}Et_2O$, or NH_4PF_6 in 1:1 stoichiometry affords respectively the N–H–N *monoprotonated* species [**2**H][X] (X = CF_3SO_3 (**4a**), BF_4 (**4b**), PF_6 (**4c**)). **4b** and **4c** were isolated in good yield (70–90%). Compound **4a** was characterized in solution.

The ^1H NMR spectra of **4a** indicate that it is symmetrical, with the NH^+ group being observed at 7.9 ppm (CD_3CN, 293 K) as a broad signal. This may be attributed to an NH^+ group interacting with the second N atom.[8a,11] Lowering the temperature to 193 K in CD_2Cl_2 shows a broadening of the signals of **4a** in ^1H and ^{13}C NMR spectra. A single signal is clearly observed for the methyl groups in the ^1H and ^{13}C NMR spectra (at $\delta = 2.5$ ppm, 243 K and $\delta = 36.9$ ppm, 193 K, respectively), suggesting that an H^+ exchange occurs between the two N atoms and that it is not blocked at low temperature. In the solid state, the ν (N^+H) (KBr) frequencies, observed in the 2400–2340 cm^{-1} range of the IR spectrum of **4c**, are also consistent with an additional hydrogen interaction with the second nitrogen.[11,12] The mass spectrum of **4b** indicates monoprotonation. It is worth noting that compound **4b** is cleanly obtained when compound **2** is reacted with the diprotonated complex **3b** with a 1:1 stoichiometry in CD_2Cl_2. The later experiment leads us to suggest that an exchange mechanism involving N^+H- - -N inter- and intramolecular interactions exists (Scheme 2). The flexibility of the $(-N(CH_2)_2O(CH_2)_2O(CH_2)_2N-)$ chain in compound **2** (vide infra) may favor this type of exchange, which is probably assisted by the presence of the oxygen atoms of the chain.[11,12] Subsequent addition of 1 equiv of $HBF_4{\cdot}Et_2O$ to the monoprotonated species affords **3b**.

Scheme 2

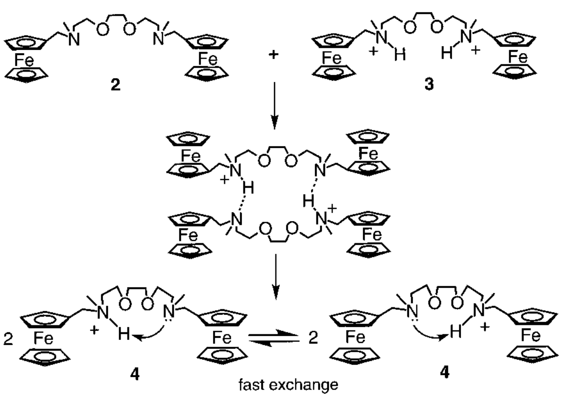

In order to compare the electrochemical properties of a methylated species with the diprotonated forms, we synthesized a dimethylated derivative of **2**. Treatment of **2** with 2 equiv of CF_3SO_3Me in CH_3CN affords $[\mathbf{2}(Me)_2][CF_3SO_3]_2$ (**5**), which was isolated in 50% yield as a yellow powder. Characterization was achieved by ^1H, ^{13}C, and $^{19}F\{^1H\}$ NMR experiments in CD_3CN.

2. Complexation Reactions. To check the bonding ability of complex **2**, we have investigated its reactivity with Na, Cu, Ag, Zn, and Hg salts.

When either 1 equiv or an excess of $NaPF_6$ salt is added to **2** in CH_3CN, the $[\mathbf{2}Na][PF_6]$ adduct (**6**) is the unique species isolated after purification. The $^{31}P\{^1H\}$, $^{19}F\{^1H\}$, and ^{23}Na NMR spectra in $CDCl_3$ allow confirmation of the complexation of the $NaPF_6$ salt, which is normally insoluble in this solvent. In the solid state, mass spectroscopy confirms that the 1:1 adduct is the unique product of the reaction.

The coordination mode of the Na^+ ion in compound **6** is not clear. Generally Na^+ requires more than four bonds in its coordination sphere; however, tetrahedral coordination with a N_2O_2 donor set is possible.[13] Na^+ presents a good affinity for N and O atoms in diazacrown ether compounds.[8b,14] In **6**

---

(7) Plenio, H.; El-Desoky, H.; Heinze, J. *Chem. Ber.* **1993,** *126*, 2403.

(8) (a) Cheney, J.; Lehn, J. M. *J. Chem. Soc., Chem. Commun.* **1972**, 487. (b) Plenio, H.; Diodone, R. *J. Organomet. Chem.* **1995**, *492*, 73.

(9) (a) Beer, P. D.; Crowe, D. B.; Ogden, M. I.; Drew, M. G. B.; Main, B. *J. Chem. Soc., Dalton Trans.* **1993**, 2107. (b) Graf, E.; Kintzinger, J. P.; Lehn, J. M.; LeMoigne, J. *J. Am. Chem. Soc.* **1982**, *104*, 1672. (c) Graf, E.; Lehn, J. M. *Helv. Chim. Acta* **1981**, *64*, 1040. (d) Graf, E.; Hosseini, M. W.; Ruppert, R.; De Cian, A.; Fischer, J. *J. Chem. Soc., Chem. Commun.* **1995**, 1505.

(10) Monitoring first this reaction with electrochemical methods allowed us to observe that addition of 2 equiv of NH_4PF_6 produces an anodic shift (220 mV) of the Fe(II)/Fe(III) couple; this could be ascribed to the formation of the adduct $[\mathbf{2}NH_4][PF_6]$.[9a]

(11) Brügge, H.-J.; Carboo, D.; von Deuten, K.; Knöchel, A.; Kopf, J.; Dreissig, W. *J. Am. Chem. Soc.* **1986**, *108*, 107.

(12) Cheney, J.; Kintzinger, J. P.; Lehn, J. M. *Nouv. J. Chim.* **1978**, *2*, 411.

(13) Crescenzi, R.; Solari, E.; Floriani, C.; Chiesi-Villa, A.; Rizzoli, C. *Inorg. Chem.* **1996**, *35*, 2413.

(14) (a) Plenio, H. *Inorg. Chem.* **1994**, *33*, 6123. (b) Plenio, H.; Diodone, R. *Inorg. Chem.* **1995**, *34*, 3964 and references therein.

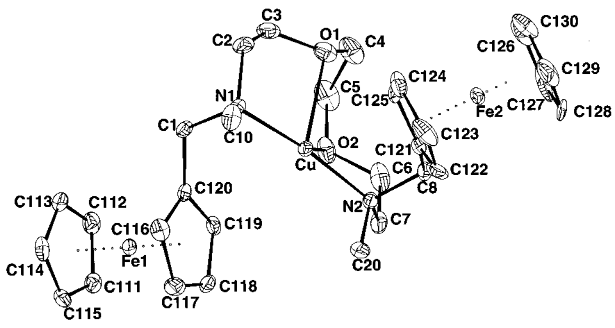

Figure 1. Molecular view of the structure of compound (**2**) (CAMERON) with 30% thermal ellipsoids.

Table 1. Crystal and Intensity Data for **7**

empirical formula: $C_{30}H_{40}N_2O_2Fe_2Cu$	formula wt: 784.96
	monoclinic, space group $P2_1/c$
$a = 11.511(2)$ Å	$T = -93$ °C
$b = 19.613(2)$ Å	λ(Mo Kα_1) = 0.710 73 Å
$c = 14.493(2)$ Å	$\rho_{calcd} = 1.59$ g cm^{-3}
$\beta = 88.32(2)$°	$\mu = 15.44$ cm^{-1}
$V = 3273.2(1)$ Å^3	$R^a = 0.034$
$Z = 4$	$R_w{}^b = 0.039$

[a] $R = \sum||F_o| - |F_c||/\sum|F_o|$. [b] $R_w = [\sum w(|F_o| - |F_c|)^2/(\sum w|F_o|^2)]^{1/2}$.

additional coordination could be provided from the PF_6 counteranion through its F atoms.[15] However, $^{31}P\{^1H\}$ (161.98 MHz, CD_2Cl_2) variable temperature NMR experiments down to 183 K do not show significant variation of the spectra, thus lending no support to this proposal (the heptuplet at −141.72 ppm is not modified). Yellow crystals of the pure compound were obtained, but they were not suitable for X-ray diffraction studies.

When treated with $CuCF_3SO_3{\cdot}0.5C_6H_6$ in 1:1 stoichiometry in CH_2Cl_2 or THF, **2** afforded the adduct [**2**Cu][CF_3SO_3] (**7**). Mass spectra show that **7** is the unique complexation adduct formed under these experimental conditions. The most important ^1H deshielding is observed for the $FcCH_2N$ protons ($\Delta\delta = 0.75$ ppm in $CDCl_3$) and is associated with a broadening of the resonances. When complex **7** is dissolved in acetonitrile, ligand **2** is displaced by the solvent. This copper complex is prone to rapid oxidation in solution in the presence of dioxygen but was found to be sufficiently stable to allow characterization.

Crystals of **7** suitable for X-ray analysis were obtained by recrystallization from a 1:3 CH_2Cl_2/Et_2O mixture. An X-ray structure determination realized at 293 K shows very large thermal ellipsoids especially for the C atoms in the ether chain; this initially hampered a good refinement of the structure ($R = 0.095$, $R_w = 0.111$). A perspective view of the molecule from data obtained at 180 K is shown in Figure 1. Selected bond lengths and interatomic angles are listed in Tables 1 and 2, respectively. **2** is symmetrically coordinated to the copper atom through its N and O donor atoms with the N−C, C−O and C−C distances within the normal ranges.[1e,16] Usual Cu−N distances (Cu−N(1) = 1.966(4) Å, Cu−N(2) = 1.953(4) Å) are observed,[3a,17a] but the Cu−O distances (Cu−O(1) = 2.517(4) Å, Cu−O(2) = 2.610(4) Å) are elongated by the ligand architecture and are close to those found in copper(II) complexes bound to a similar diazadioxa organic chain.[18,19] The consequence for the copper atom is a very distorted tetrahedral geometry with a large N(1)−Cu(1)−N(2) angle (163.1 (2)°). The presence of two nitrogen atoms in a tetrahedral environment together with the stereochemical requirement of the methyl and ferrocenyl groups may enforce this particular geometry.

Table 2. Selected Bond Lengths (Å) and Bond Angles (deg) for **7**, with Esd's in Parentheses

Bond Lengths (Å)

Cu−O(1)	2.517(4)	C(2)−C(3)	1.483(9)
Cu−O(2)	2.610(4)	C(3)−O(1)	1.419(7)
Cu−N(1)	1.966(4)	O(1)−C(4)	1.422(8)
Cu−N(2)	1.953(4)	C(4)−C(5)	1.515(9)
N(1)−C(1)	1.512(6)	C(5)−O(2)	1.431(8)
N(1)−C(2)	1.484(7)	O(2)−C(6)	1.413(7)
N(1)−C(10)	1.490(7)	C(6)−C(7)	1.50(1)
C(1)−C(120)	1.500(7)	C(7)−N(2)	1.499(8)
C(8)−C(121)	1.495(7)	N(2)−C(8)	1.515(6)

Bond Angles (deg)

O(1)−Cu−O(2)	66.4(2)	C(10)−N(1)−C(2)	108.8(4)
O(1)−Cu−N(1)	79.4(2)	Cu−N(1)−C(2)	111.4(3)
O(2)−Cu−N(1)	117.6(2)	C(1)−N(1)−C(2)	109.7(3)
O(1)−Cu−N(2)	114.2(2)	N(1)−C(2)−C(3)	113.7(4)
O(2)−Cu−N(2)	78.2(2)	C(2)−C(3)−O(1)	107.6(4)
N(1)−Cu−N(2)	163.1(2)	O(1)−C(4)−C(5)	112.0(5)
C(1)−N(1)−C(10)	108.2(4)	C(4)−C(5)−O(2)	111.5(5)
C(10)−N(1)−Cu	107.7(3)	C(5)−O(2)−C(6)	114.2(5)
C(1)−N(1)−Cu	111.0(3)	N(1)−C(1)−C(120)	110.4(3)
		N(2)−C(8)−C(121)	112.5(4)

Cu(I) and Ag(I) compounds are known[17] to prefer tetrahedral geometry, but few examples of ferrocenyl silver compounds have been reported.[1e,20] With this in mind, along with the fact that Ag(I) can accommodate N and O ligands in a tetrahedral geometry,[21,22] formation of a silver adduct of **2** was conceivable. The compound [Ag**2**][CF_3SO_3] (**8**) has been isolated in 50% yield from the 1:1 reaction of compound **2** with $AgCF_3SO_3$ in THF. Mass spectra carried out on a pure sample confirmed the proposed formula. As for the copper compound **7**, the ^1H NMR signals in $CDCl_3$ are broad, but in contrast to **7** the Ag adduct is stable in CD_3CN. ^1H NMR spectra in this solvent show a weak deshielding of the signals (0.1−0.2 ppm) when compared to those of the starting material, and they show ill-resolved multiplets for NCH_2CH_2O and $FcCH_2N$ protons. Low-temperature NMR experiments of **8** (CD_2Cl_2, 193 K) are not informative, and the complex decomposes upon heating to 333 K in CD_3CN. Attempts to crystallize **8** were unsuccessful, and a detailed mode of coordination cannot be proposed, though a structure similar to that of **7** may be suggested.

When a slight excess of $AgCF_3SO_3$ was added to a solution of **2**, the mixture turned green. This fact suggested to us that the extra silver salt could act as an oxidizing agent toward the Fe(II) centers (vide infra).

Recently, addition of $Zn(CF_3SO_3)_2$ to a solution of an aminoferrocene complex has been shown to induce the largest anodic shift ever observed for the redox potential of the Fe(II)/Fe(III) couple.[23e] With the aim of synthesizing [Fe−Zn]$^{2+}$ complexes, reaction of compound **2** with 1 equiv of $Zn(CF_3SO_3)_2$ was carried out. After purification, the diprotonated complex **3a** was identified by NMR and mass spectroscopy as the unique product of the reaction, demonstrating the easy protonation of the chain.

---

(15) Beer, P. D.; Sikanyika, H.; Blackburn, C.; McAleer, J. F.; Drew, M. G. B. *J. Chem. Soc., Dalton Trans.* **1990**, 3295.

(16) Plenio, H.; Yang, J.; Diodone, R.; Heinze, J. *Inorg. Chem.* **1994**, *33*, 4098.

(17) (a) Beer, P. D.; Crane, C. G.; Drew, M. G. B. *J. Chem. Soc., Dalton Trans.* **1991**, 3235. (b) Beer, P. D. *J. Chem. Soc., Chem. Commun.* **1986**, 1678 and references therein. (c) Greenwood, N. N.; Earnshaw, A. *Chemistry of the Elements*; Pergamon Press: Oxford, U.K., 1984; Chapter 28, p 1364.

(18) Marsch, R., E.; Bernal, Y. *Acta Crystallogr.* **1995**, *B 51*, 300.

(19) Clegg, W.; Lockhardt, J. C. *Polyhedron* **1987**, *6*, 1149.

(20) Beer, P. D.; Chen, Z.; Drew, M. G. B.; Johnson, A. O. M.; Smith, D. K.; Spencer, P. *Inorg. Chim. Acta* **1996**, *246*, 143.

(21) Dias, H. V.; Wiechang, J. *Inorg. Chem.* **1996**, *35*, 267.

(22) Smith, G.; Lynch, D. E.; Kennard, C. H. L. *Inorg. Chem.* **1996**, *35*, 2711.

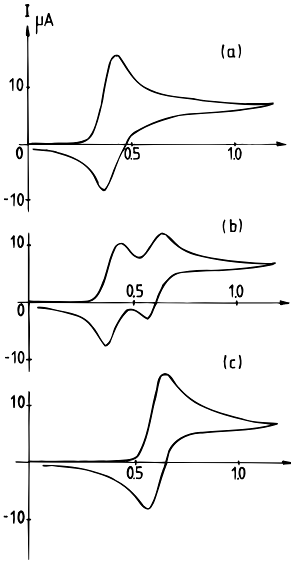

Figure 2. Cyclic voltammograms of (a) **2**, (b) **2** + 1 equiv of NH_4PF_6, and (c) **2** + 2 equiv of NH_4PF_6 at 0.1 V s^{-1}. Experimental conditions: Pt electrode (1 mm) in 0.1 mol L^{-1} solution of $^nNBu_4PF_6$ in CH_3CN, complex concentration 10^{-3} M.

To our knowledge, neutral ferrocenyl iron−zinc and iron−mercury complexes are scarce[23,24] and only a few complexes have been structurally characterized.[3d,23c,e,24a] Reaction of **2** with $ZnCl_2$ and $HgCl_2$ led us to successful isolation of the respective metal ligand complexes [$\mathbf{2}ZnCl_2$] (**9**) and [$\mathbf{2}HgCl_2$] (**10**), the elemental analyses of which suggested a 1:1 ligand:metal stoichiometry. Coordination of these units to ligand **2** also involves a weak ^1H NMR deshielding of the signals (0.2−0.3 ppm). In the case of the Zn adduct, the signals are broad and low-temperature NMR experiments indicate that complex phenomena operate in solution. To achieve a tetrahedral geometry,[3d,23c−e,24] these two metals need only two of the four donor atoms (N or O) of the amino ether chain. Due to the flexibility and the symmetry of the chain, an exchange phenomenon involving decoordination of one of the two coordinated atoms of the organic chain and simultaneous coordination of an other atom is possible.[3c,d]

3. Electrochemical studies. A. Protonated and Methylated Species 3a−c, 4a−c, and 5. Typical voltammograms of these species are presented in Figure 2. They can also be obtained by stepwise addition of an appropriate number of equivalents of reactant to an acetonitrile solution of **2**.

The electrochemical properties of the ligand **2** and of the *diprotonated* **3a−c** and *dimethylated* **5** complexes have been investigated in CH_3CN (Table 3). The waves observed in cyclic voltammograms are due to oxidation of the ferrocene part of the molecule and correspond to quasi-reversible processes. A detailed analysis of the electrochemical oxidation of compound **2** is presented in the following section.

Table 3. Electrochemical Data for Complexes **2**, **3a−c**, and **5**

compd	$E_{1/2}$ (V)	P (mV)	n	E_{p_a} (V)	ΔE_p (mV)	RI_p
2	0.38	63	2	0.43	85	1.0
3a	0.59	56	2	0.64	89	1.0
3b	0.59	58	2	0.66	99	1.0
3c	0.60	57	2	0.67	75	1.0
5	0.62	55	2	0.67	80	1.0

[a] $\Delta E_p = E_p(\text{backward}) - E_p(\text{forward}) = E_{p_c} - E_{p_a}$. $RI_p = |I_p(\text{backward})/I_p(\text{forward})| = |I_{p_{red}}/I_{p_{ox}}|$. n = number of exchanged electrons in the electrochemical process. P = slope of the linear regression of $E = f(\log |i/id - i|)$. [b] See text section 4. Conditions: [complexes], 1 mmol L^{-1}; Pt electrode; rotating electrode 1000 rpm; scan rate in cyclic voltammetry, 0.1 V s^{-1}; solvent CH_3CN, Bu_4NPF_6 (0.1 mol L^{-1}).

Concerning compound **3a**, under stationary conditions, a study of the limiting current versus the square root of the electrode rotating speed showed a linearity indicating a diffusion-controlled process ($D = 5.3 \times 10^{-6}$ cm^2 s^{-1} at 25 °C). The electron transfer rate constant $k°$ calculated by the Nicholson and Shain method[25] was close to 10^{-2} cm s^{-1}, typical of a pseudoreversible process. Two faradays per mole of complex were involved in each electrochemical oxidation process for compounds **3a−c** as measured by exhaustive electrolysis of solutions of the compounds at controlled potential (0.8 V) on a platinum grid working electrode. The initially yellow solutions turned *blue* during the electrolysis. These observations suggest that the electron transfer takes place on the ferrocene part of the molecule (the two redox centers are independent). Electrochemical reduction (at 300 mV) of the oxidized forms of **3a−c** regenerates the initial compounds. The electrochemical oxidation of these cationic complexes $[\mathbf{2}(H)_2]^{2+}$ can be written

$$[\mathbf{2}(H)_2]^{2+} \rightleftharpoons [\mathbf{2}(H)_2]^{4+} + 2e$$

Significant anodic perturbations of the ferrocenyl oxidation potentials are induced by protonation and methylation of the amine groups of the chain (205−240 mV) when compared to the parent compound **2**. These values are in the same range as those obtained for the protonation and methylation of the simple ferrocenyl amine ($C_5H_5FeC_5H_4CH_2NMe_2$): 185 and 190 mV, respectively.[16] These results indicate a comparable Fe−N distance and probably reflect the good flexibility of the organic chain, which prevents a strong Fe−N interaction. The difference in the redox shifts between related protonated **3b** and methylated **5** species is rather small and in agreement with the literature data.[16]

The voltammograms of the isolated *monoprotonated* species show, at 0.1V s^{-1}, two well-defined one-electron reversible oxidation waves of equal intensity which correspond to the presence of two different chemical environments for the ferrocene groups (for example, $E_{1/2} = 0.41$, 0.59 for **4b**): the first one is similar to that of the starting complex (vide infra), and the second one (more anodic potential value) is closer to that of the diprotonated species. Taking into account the proposed exchange phenomenon (Scheme 2), the first wave can be attributed to the nonprotonated ferrocenyl part of a molecule and the second one to the protonated part. In compounds **4a−c**, the proton exchange is rapid as discussed below, but once the nonprotonated part of the molecule has been oxidized, it is not basic enough to accept (via its N atom) the proton of the nonoxidized protonated part of the molecule. An electrostatic repulsion occurs and prevents the H^+ exchange. If the proton exchange still occurred, a single oxidation peak would be observed at ≈ 0.4 V. As we have already noted, electrochemistry appears to be a convenient tool for detecting exchange phenomena, which are not always easily or cleanly detected by other techniques.[3d]

B. Electrochemical and Chemical Oxidation of Compound 2. The electrochemical behavior of compound **2** has

---

(23) (a) Bracci, M.; Ercolani, C.; Floris, B.; Basseti, M.; Chiesi-Villa, A.; Guastini, C. *J. Chem. Soc., Dalton Trans.* **1990**, 1357. (b) Fleishmann, W.-D.; Fritz, H. P. *Z. Naturforsch.* **1973**, *28b*, 383. (c) Kawamoto, T.; Kushi, Y. *J. Chem. Soc., Dalton Trans.* **1992**, 3137. (d) Corain, B.; Longato, B.; Favero, G.; Ajo, D.; Pilloni, G.; Russo, U.; Kreissl, F. R. *Inorg. Chim. Acta* **1989**, *157*, 259. (e) Plenio, H.; Dirk, B. *Organometallics* **1996**, *15*, 4054.

(24) (a) Houlton, A.; Ibrahim, S. K.; Dilworth, J. R.; Silver, J. *J. Chem. Soc., Dalton Trans.* **1990**, 2421 and references therein. (b) Mann, K. R.; Morrison, W. H.; Hendrikson, D. N. *Inorg. Chem.* **1974**, *13*, 1180.

(25) Nicholson, R. S.; Shain, I. *Anal. Chem.* **1964**, *36*, 706.

Table 4. Electrochemical Data for Complexes **2** and **6**−**8**

compd	$E_{1/2}$ (V)	E_{p_a} (V)	E_{p_r} (V)	ΔE_p (mV)	RI_p
2	0.42	0.47	0.40	70	1.0
6	0.45	0.48	0.41	70	1.0
7[b]	0.54	0.58	0.51	70	1.0
8	0.55	0.59	0.52	70	1.0

[a] Conditions: [complexes], 1 mmol L^{-1}; Pt electrode in CH_2Cl_2, Bu_4NPF_6 (0.1 mmol L^{-1}); scan rate in cyclic voltammetry, 0.1 V s^{-1}; ΔE_p, R, I_p, and *n*, have the same signification as in Table 3. [b] An additional wave at ca. 0.69 V was also observed (see text).

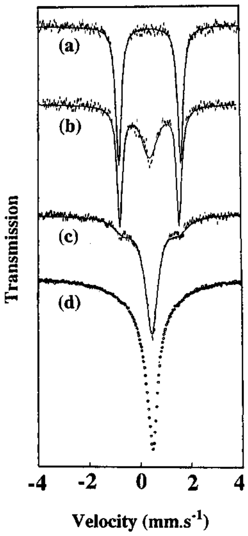

Figure 3. ^{57}Fe Mössbauer spectrum of (a) **2**, (b) **2** + 2 equiv of Ag^+, (c) **2** + 4 equiv of Ag^+, and (d) **2** + 5 equiv of Ag^+, at 80 K (isolated samples).

also been investigated in CH_2Cl_2 (Table 4). As for compound **3a** (vide supra), we have verified that the quasi-reversible oxidation process is diffusion-controlled ($D = 3.3 \times 10^{-6}$ cm^2 s^{-1} at 20 °C). About 2 faradays/mol were consumed during controlled potential electrolysis of **2** at 0.8 V, and the initial yellow solution turned *green*. In contrast with the case of the diprotonated species **3a**−**c**, or the phosphodihydrazide ligand **1**, electrochemical reduction of the oxidized species has not been possible. Passivation phenomena attributed to nonconducting deposits have been observed.

To gain a better understanding of this oxidation process, the *chemical* oxidation of compound **2** has been undertaken. Remembering the previous observation concerning reaction of **2** with a slight excess of Ag salt (vide supra), and considering its well-known oxidation properties,[26] we chose Ag^+ as oxidizing agent. When 2 equiv of Ag^+ was added to **2** in CH_2Cl_2, a green solid (similar in color to the electrochemical solution after oxidation) was obtained. Mössbauer studies of the solid (Figure 3) indicated the presence of two iron sites in equal proportion. The first one is characterized by a doublet (isomer shift, IS = 0.519(2) mm s^{-1}, quadrupole splitting, QS = 2.368(3) mm s^{-1}, at 80 K) attributed to the presence of low-spin Fe(II); the second one is a broad singlet (IS = 0.53(1) mm s^{-1}, $\Gamma/2$ = 0.39(5) mm s^{-1} at 80 K) consistent with those previously published for iron (III).[27] The green solid is not stable in solution, but its mass spectrum clearly indicates the presence of the cation **8**. The green solid corresponds thus to a mixture of products: one of them has been identified as complex **8** (solid state and solution); the other one could be the desired oxidized form of **2** responsible for the broad Fe(III) singlet observed in the Mössbauer spectrum.

Scheme 3

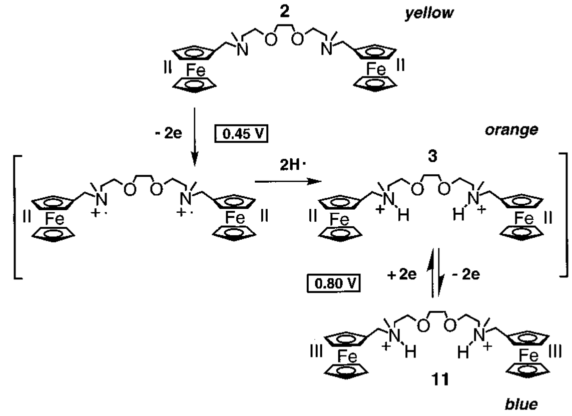

In order to verify this hypothesis, reactions of compound **2** with variable amounts of $AgCF_3SO_3$ (>2 equiv), according to a precise procedure (see Experimental Section), were undertaken. The products were isolated in solid form and analyzed by Mössbauer spectrometry (Figure 3). When 5 equiv of silver salt was added, the Mössbauer spectrum exhibited only a broad singlet[28] and the color of the isolated product was *deep blue*. Microanalyses of this sample are in agreement with the proposed formula $[\mathbf{2}(H)_2][CF_3SO_3]_4$ (**11**), where the N atoms of the chain have been protonated. Mössbauer spectra of **11** are very similar to those of the isolated product $[\mathbf{2}(Me)_2][BF_4]_4$ (**12**) obtained after electrochemical oxidation of the dimethylated compound **5** at 0.8 V in CH_3CN. Protonation of the nitrogen atoms during an oxidation reaction with a Ag salt has also been reported recently for a neutral azathiaferrocenophane.[29]

In conclusion, an excess of silver salt pushes further the complexation reaction and favors the formation of the blue oxidation product **11**. Electrochemical synthesis of this species appeared thus as a new challenge, and the *electrochemical* oxidation was reinvestigated.

A two-step oxidation was undertaken: a first electrolysis was carried out at 0.45 V (CH_3CN, Et_4NBF_4), followed by a second one at 0.8 V (Scheme 3). The value of the first potential was chosen in order to selectively oxidize compound **2** and to prevent oxidation of other products formed during this electrolysis.

During the first electrolysis (0.45 V), the *yellow* solution turned *orange* and two electrons were exchanged. After electrolysis, the cyclic voltammogram showed a wave corresponding to a quasi-reversible oxidation process ($E_{1/2}$ = 0.60 V). The intensity of this wave was nearly the same as that measured for the starting compound; an orange solution was obtained on extraction with THF. ^{1}H and ^{13}C NMR spectra of this solution proved that the diprotonated species **3b** (yellow) was the *main* product.[30]

During the second electrolysis (0.8 V), the solution turned *blue* and again two electrons were exchanged. The linear voltammogram was indicative of the presence of the Fe(III) species (cathodic current). This species can be reduced at 0.2 V to regenerate the orange solution, through a two-electron exchange. The *blue* cation $[\mathbf{2}(H)_2]^{4+}$ (**11**) has been extracted,

---

(26) See, for example: Connely, N. G.; Geiger, W. E. *Chem. Rev.* **1996**, *96*, 877.

(27) Greenwood, N. N.; Gibb, T. C. *Mössbauer Spectroscopy*; Chapman and Hall Ltd: London, 1971.

(28) Even at 4.5 K, where the magnetic relaxation is usually quenched affording the Zeeman spectrum.

(29) Kim J. S.; Bessire, A. J.; Bartsch, R. A.; Holwerda, R. A.; Czech, B. P. *J. Organomet. Chem.* **1994**, *484*, 47.

(30) A minor product which is red has been identified (NMR, <8%). It is certainly responsible for the orange color of the mixture. It is probably formed by another oxidation pathway.

Scheme 4

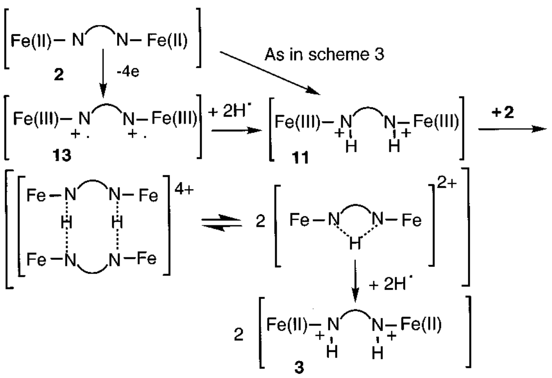

but it was impossible to prepare a sample suitable for Mössbauer experiments. However, as mentioned above, electrochemical oxidation of the dimethylated compound **5** at 0.8 V in CH_3CN allowed us to obtain the blue cation $[\mathbf{2}(Me)_2]^{4+}$ (**12**) as a sticky but more tractable oil.

Studies of the oxidation of organic amines have shown that the primary electrode process is the transfer of one electron from the lone pair of nitrogen to the anode to form a cationic radical; in wet acetonitrile, after oxidation, the original aliphatic amine R_3N is mainly recovered as the ammonium ion R_3NH^+.[31] In the case of the organometallic compound **2**, we propose the formation of a similar dicationic radical which abstracts hydrogen atoms ($H^\bullet$) from the electrochemical medium to yield the diprotonated species. Oxidation of the ferrocenyl moiety then occurs to afford the blue complex.

A minor irreversible wave detected at 1.3 V in the cyclic voltammogram of **2** can be attributed to the oxidation of the amine. This implies that, during the first electrolysis, formation of the dicationic radical occurred after oxidation of the ferrocenyl parts and rapid electron transfer from the nitrogen to the iron centers. A similar mechanism has recently been proposed by Simpson et al. for azadiferrocenyl compounds.[32] It is clear now that the two-step electrochemical oxidation of compound **2** corresponds to the following ECE (electrochemical, chemical, electrochemical) mechanism.

$$\begin{array}{llll} \mathbf{2} - 2e & \rightarrow & \mathbf{2}^{2(\bullet+)} & \mathrm{E} \\ \mathbf{2}^{2(\bullet+)} + 2H^\bullet & \rightarrow & \mathbf{3} & \mathrm{C} \\ \mathbf{3} - 2e & \rightarrow & \mathbf{11} & \mathrm{E} \end{array}$$

With respect to the result of the former electrolysis carried out at 0.8 V and affording a *green* solution, another mechanism can be proposed (Scheme 4). It involves the following steps: (a) rapid formation of the diprotonated tetracationic *blue* species **11** either by the path illustrated in Scheme 3 or after formation of the tetracationic nonprotonated species (**13**); (b) fast reaction of **11** with the starting *yellow* compound **2** to afford, through a rapid rearrangement and a new abstraction of $H^\bullet$, the more stable diprotonated dicationic complex **3**. This proposed mechanism can explain why only 2 faradays/mol (or less) is necessary under these conditions to yield **3**. Unlike the two-step electrochemical oxidation, **11** can react with **2** in solution as soon as it is formed. The *green* color observed corresponds to a mixture of **11** and **2** and/or **3**. It is worth noting that the presence of a minor iron(III) species and of the major diprotonated species **3** has been detected after electrolysis. Furthermore, the blue species **11** is not very stable in solution and decomposes, yielding a green or yellow solution (depending on the solvent) containing the diprotonated species **3**. Passivation phenomena may be ascribed to minor decomposition processes due to the nature of the tetracationic species.

A judicious choice of the oxidation potential has allowed us to prove that a selected oxidation pathway can be favored and that the diprotonated product is a key intermediate.

C. Compounds 6–8. Electrochemical results obtained for complexes **6**–**8** are gathered in Table 4.

Previous electrochemical studies on polymetallic phosphohydrazone ferrocenyl complexes have shown that the variation in the electrochemical properties of the ferrocene centers is a sensitive probe for evaluating the complexation of the ferrocenyl phosphodihydrazone ligand **1**.[3c,d] Complex **6** undergoes a quasi-reversible oxidation process at a potential value ($E_{1/2} = 0.45$ mV) that is nearly coincident with that of the free ligand **2**. This probably reveals a weak binding between **2** and Na^+. Complexes **7** and **8** undergo a reversible two-electron oxidation step in dichloromethane at potentials very close to each other (0.54 and 0.55 V), which demonstrates the lack of interaction between the two ferrocenyl centers of each of the species. Complexation of copper and silver ions in CH_2Cl_2 solution causes the two-electron oxidation of the ferrocene fragment to shift anodically by 120 and 130 mV, respectively. The $\Delta E_{1/2}$ value obtained for the copper compound is in the same range as that obtained for the diferrocenyl phosphohydrazone derivatives of copper(I).[3c,33] The $\Delta E_{1/2}$ value obtained for the silver compound is very close to that obtained for the diferrocenyl crown silver cation $[(Fc{-}L_a{-}Fc)Ag]^+$ ($L_a = -CH_2N((CH_2)_2O(CH_2)_2O(CH_2)_2)_2NCH_2-$) (110mV)[1e] but larger than that observed for the formation of the recently reported azadiferrocenyl disilver macrocyclic cation $[(Fe(C_5H_4{-}L_b{-}C_5H_4)_2Fe)Ag_2]^{2+}$ ($L_b = -CH_2NH(CH_2)_4NHCH_2-$) (45 mV) (when compared to their respective parent compounds).[20] The perturbation observed in the cyclic voltammograms is probably due to a secondary effect resulting from the close approach of silver coordinated to the nitrogen atom. The similar electrochemical behavior of **7** and **8** probably reflects the same type of phenomenon and similar coordination modes for $\mathbf{2}Cu^+$ and $\mathbf{2}Ag^+$.

Electrolyses of compounds **6**–**8** have been carried out at different oxidation potentials, producing unstable green mixtures containing diprotonated species.

4. Mössbauer Spectra of Compounds 2, 3c, and 6–8. Mössbauer studies of ferrocene derivatives have previously established correlations between QS values and the redox potential of the Fe(II)/Fe(III) couple of disubstituted ferrocenes.[34] Several groups have also used this technique in order to investigate the possible interaction of complexed cations with different ferrocene-base ligands (cryptands, macrocycles) leading to correlations between the Mössbauer parameters and the $Fe{-}M^{n+}$ internuclear distance, or the strength of this interaction.[1d,35,36]

In light of these results, Mössbauer studies of compounds **2**, **3c**, and **6**–**8** have been undertaken, the results of which are gathered in Table 5. At 297 K, no spectra are obtained for **2** and **7**. From 200 K to 4 K, the spectra for all complexes

---

(31) Ross, S. D.; Finkelstein, M.; Rudd, E. J. In *Anodic Oxidation*; Academic Press: New York, 1975; Vol. 32, Chapter 8, p 189.

(32) Spescha, M.; Duffy, N. W.; Robinson, B. H.; Simpson, J. *Organometallics* **1994**, *13*, 4895.

(33) The novel copper compound **7** also presents a wave of lower intensity at 0.69 V vs SCE resulting from the oxidation of Cu(I) as previously observed for the above mentioned iron–copper compounds.[3c]

(34) Roberts, R. M. G.; Silver, J. *J. Organomet. Chem.* **1984**, *263*, 235.

(35) Hall, C. D.; Danks, I. P.; Hammond, P. J.; Sharpe, N. W.; Thomas, M. J. K. *J. Organomet. Chem.* **1990**, *388*, 301.

(36) (a) Akabori, S.; Shibahara, S.; Habata, Y.; Sato, M. *Bull. Chem. Soc. Jpn* **1984**, *57*, 63. (b) Akabori, S.; Habata, Y.; Sato, M. *Bull. Chem. Soc. Jpn* **1984**, *57*, 68. (c) Akabori, S.; Habata, Y.; Sakamoto, Y.; Sato, M.; Ebine, S. *Bull. Chem. Soc. Jpn.* **1983**, *56*, 537.

Table 5. Least-Squares Fitted Mössbauer Data *a,b* for Compounds **2**, **3c**, and **6**−**8** at 80 K

compd	IS (mm/s)	QS (mm/s)	Γ/2 (mm/s)
2	0.527(1)	2.397(2)	0.128(2)
3c	0.510(2)	2.390(5)	0.115(4)
6	0.520(1)	2.382(2)	0.116(2)
7	0.523(1)	2.389(2)	0.121(1)
8	0.520(1)	2.378(2)	0.133(1)

[a] IS: isomer shift. QS: quadrupole splitting. Γ/2: half-hight width of line. [b] With their statistical standard deviation given in parentheses; isomer shift values refer to metallic iron at 300 K.

examined consist of a temperature independent quadrupole split doublet, typical of low-spin Fe(II), which presents approximately the same parameters as those of ligand **2** at 80 K (IS = 0.527(1) mm s^{-1}, QS = 2.397(2) mm s^{-1}).

From these data, we can conclude that protonation or complexation reactions have no effect on the Mössbauer parameters observed for compound **2** and that no direct interaction occurs between the complexed cation and the iron center. In each molecule, both iron sites are in the same local environment. Considering now the different oxidation potentials observed for these molecules, it is clear that no correlation with Mössbauer parameters can be made.

Conclusion

As for the phosphodihydrazone complex **1**, complex **2** is an efficient ligand for many metals; 1:1 adducts are obtained with small (Na^+) and larger cations (Ag^+) and also with neutral units (MCl_2, M = Zn, Hg). This may be due to the relative flexibility of the organic chain as shown for the copper compound (X-ray structure). NMR, Mössbauer, and electrochemical data show that all new molecules are symmetric in nature. Cyclic voltammetry has shown that the complexation reactions induce small anodic shifts of the redox potential of the Fe(II)/Fe(III) couple for the cationic species.

Ligand **2** can be easily and cleanly mono- or diprotonated. The synthesis of the monoprotonated species provides us the opportunity to electrochemically detect a proton exchange between the two nitrogen atoms of the ligand.

The two-step electrochemical oxidation of **2** can lead to the same cation **11** as its chemical oxidation by $AgCF_3SO_3$ (5 equiv). The complementary use of different techniques (electrochemistry, NMR, Mössbauer, and so on) has allowed us to propose an ECE mechanism for this oxidation process.

This study shows that, in contrast to **1**, ligand **2** cannot be recovered after successive controlled electrochemical oxidation/reduction processes of a (**2**)M^+ derivative. Unlike the phosphohydrazone chain, the novel N_2O_2 organic chain has a key role during the oxidation process and is protonated. The use of this ligand for electrochemical recognition of cations would require its deprotonation after oxidation of the complexed cationic species in order to be recycled.

Experimental Section

Tetrahydrofuran and diethyl ether were distilled over sodium/benzophenone, dichloromethane was distilled over P_2O_5, and pentane and CH_3CN were distilled over CaH_2 and stored under argon. $[CH_3NH(CH_2)_2O(CH_2)-]_2$ (Acros), HBF_4 (85% in Et_2O), HCF_3SO_3 (98%), $MeCF_3SO_3$, NH_4PF_6 (95%), $NaPF_6$ (98%), $Ag(CF_3SO_3)$ (99+%), $Zn(CF_3SO_3)_2$ (98%) (Aldrich), anhydrous $ZnCl_2$ (98%) (Prolabo), $HgCl_2$ (Ega Chimie), $Cu(CF_3SO_3)\cdot 0.5C_6H_6$ (90%) (Fluka), and $FcCH_2NMe_2$ (Lancaster) were used without further purification. $FcCH_2NMe_3I$[37] and $[(C_5H_5)Fe(C_5H_4CH_2NCH_3(CH_2)_2OCH_2-)]_2$[4] (**2**) were prepared according to published procedures. All syntheses were performed under a nitrogen or argon atmosphere using standard Schlenk tube techniques. IR spectra were recorded on a Perkin-Elmer 983 spectrophotometer. Samples were run as KBr pellets prepared in a glovebox. Elemental analyses were carried out on a Perkin-Elmer 2400 B analyzer at the L. C. C. Microanalytical Laboratory in Toulouse. Mass spectra (fast atom bombardment, FAB>0; or desorption chemical ionization, DCI) were performed on a Nermag R10 at the Service Commun de Spectrometrie de Masse de l'Université Paul Sabatier et du CNRS in Toulouse. ^1H, ^{13}C, and ^{31}P NMR spectra have been performed on Bruker AC 80, AC 200, AM 250, and AMX 400 spectrometers. ^{31}P NMR spectra are referenced to external 85% H_3PO_4 in D_2O, ^1H and ^{13}C NMR spectra are referenced to tetramethylsilane,^{19}F NMR spectra are referenced to external CF_3COOH (10% in C_6D_6), and ^{23}Na NMR spectra are referenced to NaCl, 4 M in D_2O. Variable-temperature and selective decoupling experiments were carried out on an AMX 400 spectrometer equipped with a multinuclear probe. The observation and decoupling frequencies were in the range 400.13 MHz for ^1H, 161.98 MHz for ^{31}P, 100.62 MHz for ^{13}C, and 105.84 MHz for ^{23}Na.

Electrochemical Studies. Electrochemical measurements were carried out with a home-made potentiostat using an interfacing hardware with a PC-compatible microcomputer. The positive feedback or interrupt method was used to compensate for IR drop. A conventional electrochemical cell was used, including three electrodes: a Pt disk (diameter 1 mm) working electrode, a Pt wire auxiliary electrode, and a SCE reference electrode for cyclic voltammetry (scan rate, 0.1 V s^{-1}). A rotating disk electrode of Pt with a diameter of 2 mm (EDI Tacussel) was used for analytical purposes (scan rate, 5 mV s^{-1}; rotation speed, 1000 rpm). For electrolysis experiments, a Pt grid or a Pt foil was used. The reference electrode consisted of an SCE separated from the solution by a bridge compartment filled with the same solvent and supporting electrolyte solution. All solutions measured were 1.0×10^{-3} M in the organometallic complex and 0.1 M in supporting electrolyte. Analogous solutions were used for controlled potential coulometry. The supporting electrolyte Bu_4NPF_6 or Et_4NBF_4 (Aldrich analytical grade) was used as received. Dichloromethane (SDS, purex) was refluxed on CaH_2 and distilled under an argon atmosphere prior to use. CH_3CN (Aldrich 99+%) was dried over molecular sieves. The solutions were degassed by bubbling argon during experiments. With the above reference, $E° = 0.42$ V vs SCE was obtained for 1 mM ferrocene.

Mössbauer Studies. Measurements were obtained on a constant-acceleration conventional spectrometer with a 25 mCi source of ^{57}Co (Rh matrix). Isomer shift values (IS) throughout the paper are given with respect to metallic iron at room temperature. The absorber was a sample of 80 mg of microcrystalline powder enclosed in a 2 cm diameter cylindrical plastic sample holder, the size of which had been determined to optimize the absorption. Variable-temperature spectra were obtained in the 300−4.2 K range, by using a MD 306 Oxford cryostat, the thermal scanning being monitored by an Oxford ITC4 servocontrol device (±0.1 K accuracy). A least-squares computer program[38] was used to fit the Mössbauer parameters and determine their standard deviations of statistical origin (given in parentheses).

$[(C_5H_5)Fe(C_5H_4CH_2N(CH_3)(CH_2)_2OCH_2-)]_2$ (2). ^1H NMR (400 MHz, $CDCl_3$): δ 2.20 (s, 6H, CH_3), 2.54 (t, $^3J = 6.1$ Hz, 4H, NCH_2CH_2O), 3.45 (s, 4H, $FcCH_2N$), 3.55 (t, $^3J = 6.1$ Hz, 4H, NCH_2CH_2O), 3.58 (s, 4H, OCH_2CH_2O), 4.11 (br s), 4.16(br s) (18H, $C_5H_5FeC_5H_4$). $^{13}C\{^1H\}$ NMR (100.62 MHz, $CDCl_3$): δ 42.17 (s, CH_3), 55.41 (s, NCH_2CH_2O), 57.57 (s, $FcCH_2N$), 69.49 (s, NCH_2CH_2O), 68.40 (s, C_5H_5), 67.94, 70.23, 82.64 (each s, C_5H_4), 70.31 (s, OCH_2CH_2O). ^1H NMR (200 MHz, $CDCl_3$): δ 2.18 (s, 6H, CH_3), 2.51 (t, 4H, $^3J = 5.3$ Hz, NCH_2CH_2O), 3.42 (s, 4H, $FcCH_2N$), 3.53 (t, $^3J = 5.3$ Hz, NCH_2CH_2O), 3.56 (s, 4H, OCH_2CH_2O), 4.08 (br s, 10H, C_5H_5), 4.08, 4.14 (m, 8H, C_5H_4). MS-DCI: 573 $[M + H]^+$.

Synthesis of $[2(H)_2][CF_3SO_3]_2$ (3a). Method A. 168 mg (1.1 mmol) of HCF_3SO_3 was added to a solution of **2** (310 mg, 0.5 mmol) in 5 mL of CH_3CN. The mixture was stirred for 0.5 h, and the solvent was evaporated to dryness. The yellow oil obtained was purified by diffusion in a 2:3 CH_2Cl_2/pentane mixture. The solvent was filtered

---

(37) Lednicer, D.; Hauser, C. R. *Org. Synth.* **1960**, *40*, 434.

(38) Varret, F. *Proceedings of the International Conference on Mössbauer Effect Applications, Jaipur, India, 1981*; Indian National Science Academy: New Delhi, **1982**.

off and the oil dried under vacuum: 448 mg, 95% yield. ^{1}H NMR (400 MHz, CD$_3$CN): δ 2.77 (m, 6H, CH$_3$), 3.21 (dm, 4H, NC*H*$_2$CH$_2$O), 3.66 (s, 4H, OCH$_2$CH$_2$O), 3.75 (t, 4H, J = 15.0 Hz, NCH$_2$C*H*$_2$O), 4.23 (br s, 4H, FcCH$_2$N), 4.30 (s, 10 H, C$_5$H$_5$), 4.39, 4.50, 4.52 (8H, each br s, C$_5$H$_4$), 7.42 (s, 2H, NH). ^{13}C{^{1}H} NMR (100.62 MHz, CD$_3$CN): δ 40.14 (s, CH$_3$), 54.21, 54.26 (each s, NC*H*$_2$CH$_2$O), 57.43 (s, FcCH$_2$N), 64.39 (s, NCH$_2$C*H*$_2$O), 69.72 (s, C$_5$H$_5$), 70.58, 70.70, 71.92, 72.20, 74.11 (each s, C$_5$H$_4$), 70.46 (s, OCH$_2$CH$_2$O); (CD$_2$Cl$_2$, 193 K): δ 119.4 (q, J_{CF} = 319 Hz). MS-FAB: 723 [M − CF$_3$SO$_3$]$^+$, 573 [M − 2CF$_3$SO$_3$ − H]$^+$. Anal. Calcd for **3a**, C$_{32}$H$_{42}$N$_2$O$_8$S$_2$F$_6$Fe$_2$: C, 44.05; H, 4.85; N, 3.21. Found: C, 43.72; H, 4.90; N, 3.25.

Method B. A mixture of **2** (330 mg, 0.58 mmol) and 1 equiv of Zn(CF$_3$SO$_3$)$_2$ (213 mg, 0.59 mmol) was dissolved in THF (13 mL). The solution was stirred for 48 h at room temperature (20 °C). The solution was filtered and the solvent evaporated to dryness. The orange residue was dissolved in CH$_2$Cl$_2$ (15 mL). The solution was filtered and evaporated to dryness and the residue washed with pentane (2 × 15 mL) and dried under vacuum.

Synthesis of [2(H)$_2$][BF$_4$]$_2$ (3b). Two equivalents of HBF$_4$·Et$_2$O was syringed into a solution of **2** (340 mg, 0.59 mmol) in CH$_2$Cl$_2$ (10 mL). The mixture was stirred for 1 h at 20 °C. The solvent was evaporated to dryness under vacuum, and the yellow product was washed with diethyl ether (2 × 20 mL) and pentane (2 × 20 mL): 430 mg, 97% yield. ^{1}H NMR (200 MHz, CD$_3$CN): δ 2.83 (m, J = 2.6 Hz, 6H, CH$_3$), 3.27 (dm, 4H, NC*H*$_2$CH$_2$O), 3.71 (s, 4H, OCH$_2$CH$_2$O), 3.80 (t, J = 4.9 Hz, 4H, NCH$_2$C*H*$_2$O), 4.35 (m, 14H, FcCH$_2$N and C$_5$H$_5$), 4.45, 4.55 (each br s, 8H C$_5$H$_4$), 7.00 (s, 2H, NH). ^{13}C NMR (62.9 MHz, CD$_3$CN): δ 39.9 (q, J_{CH} = 144 Hz, CH$_3$), 54.1 (t, J_{CH} = 145 Hz, NC*H*$_2$CH$_2$O), 57.3 (t, J_{CH} = 147 Hz, FcCH$_2$N), 64.0 (t, J_{CH} = 146 Hz, NCH$_2$C*H*$_2$O), 69.4 (m, $^1J_{\mathrm{CH}}$ = 176 Hz), 70.3 (m, $^1J_{\mathrm{CH}}$ = 177 Hz), 71.7 (m, $^1J_{\mathrm{CH}}$ = 176 Hz), 73.9 (s) (C$_5$H$_5$FeC$_5$H$_4$), 70.3 (t, J_{CH} = 143 Hz, OCH$_2$CH$_2$O). ^{19}F{^{1}H} NMR (188.3 MHz, CD$_3$CN): δ −69.9 (s). MS-FAB: 661 [M − BF$_4$]$^+$, 573 [M − 2BF$_4$ − H]$^+$. Anal. Calcd for **3b**, C$_{30}$H$_{42}$N$_2$O$_2$B$_2$F$_8$Fe$_2$: C, 48.17; H, 5.66; N, 3.75. Found: C, 47.78; H, 5.84; N, 3.66.

Synthesis of [**2(H)$_2$][BF$_4$]$_2$ (3c)**. A mixture of 2 equiv of NH$_4$PF$_6$ (194 mg, 1.19 mmol) and 1 equiv of **2** (300mg, 0.52 mmol) was dissolved in CH$_3$CN (10 mL) and the reaction mixture vigorously stirred for 1 h. The solvent was evaporated to dryness, and the residue was diluted in CH$_2$Cl$_2$ (10 mL) and purified by slow filtration and evaporation of the solvent. The yellow powder obtained was washed with pentane and dried under vacuum: 410 mg, 88% yield. ^{1}H NMR (200 MHz, CD$_2$Cl$_2$, 297 K): δ 2.84 (s, 6H, CH$_3$), 3.16 (dm, 4H, NC*H*$_2$CH$_2$O), 3.70 (s, 4H, OCH$_2$CH$_2$O), 3.72 (t, J = 5.1 Hz, 4H, NCH$_2$C*H*$_2$O), 4.26 (s br, 4H, FcCH$_2$N), 4.37 (br s), 4.38 (br s), 4.46 (m) (18H, C$_5$H$_5$FeC$_5$H$_4$), 6.64 (br s , 2H, NH). ^{13}C NMR (100.62 MHz, CD$_2$Cl$_2$, 297 K): δ 40.28 (q, J_{CH} = 143 Hz, CH$_3$), 53.87 (t, J_{CH} = 142 Hz, NC*H*$_2$CH$_2$O), 57.71 (t, J_{CH} = 146 Hz, FcCH$_2$N), 64.25 (t, J_{CH} = 156 Hz, NCH$_2$C*H*$_2$O), 69.38 (d, J_{CH} = 176 Hz), 70.43 (d, J_{CH} = 184 Hz), 71.57 (d, J_{CH} = 183 Hz), 73.20 (s) (C$_5$H$_5$FeC$_5$H$_4$), 69.67 (t, J_{CH} = 177 Hz, OCH$_2$CH$_2$O). ^{31}P{^{1}H} NMR (81.02 MHz, CDCl$_3$): δ −144.0 (h, J_{PF} = 713 Hz); (CD$_3$CN) δ −139.1 (h, J_{PF} = 707 Hz). ^{19}F{^{1}H} NMR (188.30 MHz, CD$_3$CN): δ 8.6 (d, J_{PF} = 707 Hz). MS-FAB: 719 [M − PF$_6$]$^+$, 573 [M − 2PF$_6$ − H]$^+$. IR (KBr, ν, cm^{-1}): 3199 (ν NH$^+$). Anal. Calcd for **3c**, C$_{30}$H$_{42}$N$_2$O$_2$P$_2$F$_{12}$Fe$_2$: C, 41.66; H, 4.90; N, 3.24. Found: C, 42.09; H, 4.93 N, 3.31.

Synthesis of [2H][CF$_3$SO$_3$] (4a). Compounds **4a**−**c** are hygroscopic. HCF$_3$SO$_3$ (1 equiv) was added to a solution of **2** (1 equiv) in CD$_3$CN. The mixture reacted for 1 h, and the solvent was evaporated under vacuum. The product was then dissolved in CD$_2$Cl$_2$. ^{1}H NMR (400 MHz, CD$_2$Cl$_2$): δ 2.57 (s, 6H, CH$_3$), 2.95 (t, ^3J = 5.1 Hz, 4H, NC*H*$_2$CH$_2$O), 3.67 (s, 4H, OCH$_2$CH$_2$O), 3.70 (t, ^3J = 5.1 Hz, 4H, NCH$_2$C*H*$_2$O), 3.96 (s, 4H, FcCH$_2$N), 4.19 (s, 10H, C$_5$H$_5$), 4.27, 4.36 (each "t", J = 1.8 Hz, 8H, C$_5$H$_4$), 7.92 (s, 1H, NH). ^{13}C{^{1}H} NMR (100.62 MHz, CD$_2$Cl$_2$): δ 37.65 (s, CH$_3$), 51.22 (s, NC*H*$_2$CH$_2$O), 54.50 (s, FcCH$_2$N), 63.08 (br s , NCH$_2$C*H*$_2$O), 66.09, 66.59, 69.57, 73.20 (each br s, C$_5$H$_5$FeC$_5$H$_4$), 67.40 (br s , OCH$_2$CH$_2$O), 117.9 (q, J_{CF} = 320 Hz, CF$_3$SO$_3$).

Synthesis of [2H][BF$_4$] (4b). Compound **2** (300 mg, 0.52 mmol) was treated in a similar manner to **3b**, with 1 equiv of HBF$_4$·Et$_2$O (99.2 mg, 0.52 mmol). The product is a yellow brown oil: 310 mg, 90% yield. ^{1}H NMR (200 MHz, CD$_3$CN): δ 2.59 (s, 6H, CH$_3$), 2.99 (t, ^3J = 4.5 Hz, 4H, NC*H*$_2$CH$_2$O), 3.69 (s, 4H, OCH$_2$CH$_2$O), 3.76 (t, ^3J = 4.5 Hz, 4H, NCH$_2$C*H*$_2$O), 4.01 (s, 4H, FcCH$_2$N), 4.31 (s, 10H, C$_5$H$_5$), 4.37, 4.50 (each "t", J = 1.8 Hz, 8H, C$_5$H$_4$), 8.20 (s, 1H, NH). ^{13}C NMR (62.9 MHz, CDCl$_3$): δ 40.4 (q, J_{CH} = 142 Hz, CH$_3$), 53.8 (t, J_{CH} = 138 Hz, NC*H*$_2$CH$_2$O), 57.1 (t, J_{CH} = 141 Hz, FcCH$_2$N), 66.0 (t, J_{CH} = 137 Hz, NCH$_2$C*H*$_2$O), 68.8 (m, $^1J_{\mathrm{CH}}$ = 176 Hz), 69.80 (m, $^1J_{\mathrm{CH}}$ = 176 Hz), 71.0 (m, $^1J_{\mathrm{CH}}$ = 181 Hz), 76.2 (s) (C$_5$H$_5$FeC$_5$H$_4$), 70.0 (t, J_{CH} = 138 Hz, OCH$_2$CH$_2$O). ^{19}F{^{1}H} NMR (188.30 MHz, CD$_3$CN): δ −69.9 (s). MS-FAB: *m/z* 660 [M]$^+$, 661 [M + H]$^+$, 573 [M − BF$_4$]$^+$. Anal. Calcd for **4b**, C$_{30}$H$_{41}$N$_2$O$_2$BF$_4$Fe$_2$: C, 54.58; H, 6.26; N, 4.24. Found: C, 54.15; H, 6.33 N, 3.89.

Synthesis of [2H][PF$_6$] (4c). A mixture of 1 equiv of **2** (380 mg, 0.66 mmol) and 1 equiv of NH$_4$PF$_6$ (115 mg, 0.70 mmol) was dissolved in CH$_3$CN (12 mL). The solution was stirred for 15 h. After a treatment similar to that for **3c**, the product was obtained as a yellow powder: 450 mg, 94% yield. ^{1}H NMR (200 MHz, CD$_3$CN): δ 2.47 (s, 6H, CH$_3$), 2.86 (t, ^3J = 5.6 Hz, 4H, NC*H*$_2$CH$_2$O), 3.69 (s, 4H, OCH$_2$CH$_2$O), 3.71 (t, ^3J = 5.6 Hz, 4H, NCH$_2$C*H*$_2$O), 3.84 (s, 4H, FcCH$_2$N), 4.29 (s, 10H, C$_5$H$_5$), 4.34, 4.40 (each "t", J = 1.8 Hz, 8H, C$_5$H$_4$), 7.8 (br s, 1H, NH). ^{31}P{^{1}H} NMR (81.0 MHz, CD$_3$CN): δ −139.1 (h, J_{PF} = 707 Hz). ^{19}F{^{1}H} NMR (188.30 MHz, CD$_3$CN): δ 8.5 (d, J_{PF} = 707 Hz). Anal. Calcd for **4c**, C$_{30}$H$_{42}$N$_2$O$_2$PF$_6$Fe$_2$: C, 50.13; H, 5.75; N, 3.90. Found: C, 50.51; H, 6.16 N, 4.01. IR (KBr, ν, cm^{-1}): 2402, 2360 , 2343 (ν NH$^+$).

Synthesis of [2(Me)$_2$][CF$_3$SO$_3$]$_2$ (5). MeCF$_3$SO$_3$ (2 equiv, 267 mg, 1.63 mmol) were syringed into a solution of **2** (460 mg, 0.80 mmol) in CH$_3$CN (17 mL). The solution was stirred for 15 h, and 30 mL of diethyl ether was slowly added. After diffusion, the solvent was filtered off, and the brown residue obtained was washed with ether and pentane and dried under vacuum, affording a yellow powder: 360 mg, 50% yield. ^{1}H NMR (400 MHz, CD$_3$CN): δ 2.96 (s, 12H, CH$_3$), 3.38 (m, 4H, NC*H*$_2$CH$_2$O), 3.71 (s, 4H, OCH$_2$CH$_2$O), 3.89 (br s , 4H, NCH$_2$C*H*$_2$O), 4.30 (s, 10H, C$_5$H$_5$), 4.43, 4.54 (8H, each "t", J = 1.8 Hz, C$_5$H$_4$), 4.46 (br s, 4H, FcCH$_2$N). ^{13}C NMR (62.9 MHz, CD$_3$CN): δ 50.2 (q, J_{CH} = 145 Hz, NCH$_3$), 62.5 (t, J_{CH} = 141 Hz NC*H*$_2$CH$_2$O), 64.4 (t, J_{CH} = 142 Hz, FcCH$_2$N), 66.8 (t, J_{CH} = 150 Hz, NCH$_2$C*H*$_2$O), 69.4 (m, $^1J_{\mathrm{CH}}$ = 176 Hz), 70.6 (m, $^1J_{\mathrm{CH}}$ = 178 Hz), 72.6 (m, $^1J_{\mathrm{CH}}$ = 178 Hz) (C$_5$H$_5$FeC$_5$H$_4$), 70.0 (t, J_{CH} = 142 Hz, OCH$_2$CH$_2$O). ^{19}F{^{1}H} NMR (188.30 MHz, CD$_3$CN): δ 2.1 (s). MS-FAB: 751 [M − CF$_3$SO$_3$]$^+$. Anal. Calcd for **5**, C$_{34}$H$_{46}$N$_2$O$_8$F$_6$S$_2$Fe$_2$: C, 45.33; H, 5.15; N, 3.11. Found: C, 45.08; H, 4.91 N, 3.03.

Synthesis of [2Na][PF$_6$] (6). A solution of 174.7 mg (1.04 mmol) of NaPF$_6$ in CH$_3$CN (6 mL) was added to a solution of **2** (530 mg, 0.93 mmol) in CH$_3$CN (25 mL). The mixture was stirred for 40 h, the solution was filtered, and the solvent was evaporated to dryness. The residue was dissolved in CH$_2$Cl$_2$ (10 mL). After filtration, the solvent was evaporated under vacuum and the product was washed with pentane (2 × 10 mL), dried under vacuum, and obtained as a yellow powder: 507 mg, 74% yield. ^{1}H NMR (200 MHz, CDCl$_3$): δ 2.15 (s, 6H, CH$_3$), 2.56 (t, 4H, ^3J = 5.3 Hz, NC*H*$_2$CH$_2$O), 3.43 (s, 4H, NCH$_2$Fc), 3.52 (t, 4H, ^3J = 5.3 Hz, 4H, NCH$_2$C*H*$_2$O), 3.58 (s, 4H, OCH$_2$CH$_2$O), 4.12, 4.14 (each s, 18 H, C$_5$H$_5$FeC$_5$H$_4$). ^{13}C NMR (62.9 MHz, CDCl$_3$, 297 K): δ 40.8 (q, J_{CH} = 136 Hz, CH$_3$), 55.4 (t, J_{CH} = 132 Hz, NC*H*$_2$CH$_2$O), 57.3 (t, J_{CH} = 133 Hz, FcCH$_2$N), 67.2 (t, J_{CH} = 139 Hz, NCH$_2$C*H*$_2$O), 68.4 (m, $^1J_{\mathrm{CH}}$ = 173 Hz), 68.6 (m, $^1J_{\mathrm{CH}}$ = 175 Hz), 70.3 (m, $^1J_{\mathrm{CH}}$ = 175 Hz), 81.0 (br s) (C$_5$H$_5$FeC$_5$H$_4$), 69.2 (t, J_{CH} = 142 Hz, OCH$_2$CH$_2$O). ^{31}P{^{1}H} NMR (81.02 MHz, CDCl$_3$): δ −144.0 (h, J_{PF} = 712 Hz). ^{19}F{^{1}H} NMR (188.30 MHz, CDCl$_3$): δ 3.2 (d, J_{PF} = 712 Hz). ^{23}Na{^{1}H} NMR (105.84 MHz, CD$_2$Cl$_2$): δ −8.9 (br s). MS-FAB: 718 [M − Na + H]$^+$, 595 [M − PF$_6$]$^+$, 573 [M − NaPF$_6$+H]$^+$. Anal. Calcd for **6**, C$_{30}$H$_{40}$N$_2$O$_2$PF$_6$NaFe$_2$: C, 48.64; H, 5.45; N, 3.78. Found: C, 48.77; H, 5.61; N, 3.73.

Synthesis of [2Cu][CF$_3$SO$_3$] (7). A mixture of Cu(CF$_3$SO$_3$)·0.5C$_6$H$_6$ (143 mg, 0.51 mmol) and 1 equiv of **2** (280 mg, 0.49 mmol) was prepared in a glovebox and dissolved in 15 mL of THF. A precipitate appeared rapidly. After 2 h, the yellow solid was filtered off, washed with THF (5 mL) and pentane (2 × 15 mL), and dried under vacuum: 375 mg, 98% yield. ^{1}H NMR (200 MHz, CDCl$_3$): δ 2.20 (br s, 6H, CH$_3$), 2.71 (br s, 4H, NC*H*$_2$CH$_2$O), 3.73 (br s, 8H, OCH$_2$CH$_2$O and NCH$_2$C*H*$_2$O), 4.16, 4.18 (br s, 22H, C$_5$H$_5$FeC$_5$H$_4$ and FcCH$_2$N). MS-FAB: *m/z* 784 [M]$^+$, 635 [M − CF$_3$SO$_3$]$^+$. IR (KBr, ν, cm^{-1}): 1268, 1031, 638 (ν CF_3SO_3). Anal. Calcd for **7**, $C_{31}H_{40}N_2O_5SF_3Fe_2Cu$: C, 47.45; H, 5.14; N, 3.57. Found: C, 47.41; H, 5.00 N, 3.51.

Synthesis of $[2Ag][CF_3SO_3]$ (8). A light-protected mixture of Ag(CF_3SO_3) (184 mg, 0.72 mmol) and **2** (410 mg, 0.72 mmol) was prepared in a glovebox; 15 mL of THF was rapidly added. The mixture was stirred for 15 h. After filtration, the solution was evaporated to dryness and the orange powder was washed with pentane and dried under vacuum: 310 mg, 52% yield. ^1H NMR (400 MHz, CD_3CN): δ 2.40 (s, 6H, CH_3), 2.76 (br s, 4H, NCH_2CH_2O), 3.44 (br s, 4H, $FcCH_2N$), 3.63 (s, 4H, OCH_2CH_2O), 3.66 (t, $J = 4.9$ Hz, 4H, NCH_2CH_2O), 4.22, 4.30 (each br s, 18H, $C_5H_5FeC_5H_4$). ^{13}C NMR (62.9 MHz, CD_3CN): δ 44.9 (q, $J_{CH} = 133$ Hz, NCH_3), 59.0 (t, $J_{CH} = 136$ Hz), 59.8 (t, $J_{CH} = 137$ Hz), 65.4 (t, $J_{CH} = 142$ Hz), 69.4 (t, $J_{CH} = 143$ Hz) (NCH_2CH_2O, OCH_2CH_2O NCH_2CH_2O, $FcCH_2N$), 69.1 (m $^1J_{CH} = 176$ Hz), 69.5 (m, $^1J_{CH} = 176$ Hz), 70.8 (m, $^1J_{CH} = 175$ Hz), 82.8 (s) ($C_5H_5FeC_5H_4$). MS-FAB: *m/z* 828 $[M]^+$, 679 $[M - CF_3SO_3]^+$. IR (KBr, ν, cm^{-1}): 1268, 1032, 641 (ν, CF_3SO_3). Anal. Calcd for **8**, $C_{31}H_{40}N_2O_5SF_3Fe_2Ag$: C, 44.93; H, 4.87; N, 3.38. Found: C, 44.82; H, 4.88 N, 3.37.

Synthesis of $[2ZnCl_2]$ (9). A 400 mg (0.70 mmol) sample of **2** was dissolved in 20 mL of THF, and 95 mg (0.70 mmol) of $ZnCl_2$ was added to the orange solution. The mixture was stirred for 20 h at 60 °C. After filtration, pentane (40 mL) was added. After filtration and evaporation to dryness, the yellow product obtained was washed with pentane and dried under vacuum: 479 mg, 97% yield. ^1H NMR (200 MHz, $CDCl_3$): δ 2.39 (s, 6H, CH_3), 2.76 (br s, 4H, NCH_2CH_2O), 3.73, 3.80 (br s, 12H, NCH_2CH_2O, $FcCH_2N$, OCH_2CH_2O), 4.14, 4.22 (each br s, 18H, $C_5H_5FeC_5H_4$). $^{13}C\{^1H\}$ NMR (50.3 MHz, $CDCl_3$): δ 40.6 (s, NCH_3), 53.9, 57.0, 65.3, 70.2 (each br s, NCH_2CH_2O, $FcCH_2N$, OCH_2CH_2O, NCH_2CH_2O), 69.1, 69.6, 71.5 (each s, $C_5H_5FeC_5H_4$). MS-FAB: $[M + H]^+$ 709. MS-DCI: $[M + H]^+$ 709. Anal. Calcd for **9**, $C_{30}H_{40}N_2O_2Fe_2ZnCl_2$: C, 50.85; H, 5.69; N, 3.95. Found: C, 51.23; H, 6.03; N, 3.83.

Synthesis of $[2HgCl_2]$ (10). A mixture of 1 equiv of $HgCl_2$ (204 mg, 0.75 mmol) and 1 equiv of **2** (430 mg, 0.75 mmol) was rapidly dissolved in 20 mL of THF. The mixture was stirred for 29 h at 60 °C, and the solution was filtered and evaporated to dryness. After diffusion in a CH_2Cl_2/pentane mixture, the solid was washed with pentane and dried under vacuum, yielding an orange powder: 600 mg, 95% yield. ($ZnCl_2$ and $HgCl_2$ were weighed under argon.) ^1H NMR (200 MHz, $CDCl_3$): δ 2.33 (s, 6H, CH_3), 2.71 (br s, 4H, NCH_2CH_2O), 3.63 (br s, 4H, $FcCH_2N$ or OCH_2CH_2O), 3.70 (t, $J = 5.6$ Hz, 4H, NCH_2CH_2O), 3.71 (br s, 4H, $FcCH_2N$ or OCH_2CH_2O), 4.13, 4.23 (each m, 18H, $C_5H_5FeC_5H_4$). ^{13}C NMR (62.9 MHz, $CDCl_3$): δ 41.5 (q, $J_{CH} = 136$ Hz, NCH_3), 55.2, (t, $J_{CH} = 138$ Hz), 57.5 (t, $J_{CH} = 138$ Hz), 68.0 (t, $J_{CH} = 136$ Hz), 70.2 (t, $J_{CH} = 135$ Hz) (NCH_2CH_2O, $FcCH_2N$, OCH_2CH_2O, and NCH_2CH_2O), 68.5 (m, $^1J_{CH} = 176$ Hz) , 68.6 (m, $^1J_{CH} = 176$ Hz), 70.7 (m, $^1J_{CH} = 174$ Hz) ($C_5H_5FeC_5H_4$). MS-FAB: *m/z* 844 $[M]^+$, 809 $[M - Cl]^+$. MS-DCI: 809 $[M - Cl]^+$. Anal. Calcd for **10**, $C_{30}H_{40}N_2O_2Fe_2HgCl_2$: C, 42.70; H, 4.78; N, 3.32. Found: C, 42.71; H, 4.79; N, 3.26.

Chemical Oxidation of 2: **Synthesis of $[2(H)_2][CF_3SO_3]_4$ (11)**. Experiments were carried out in the absence of light, and reactants were weighed in a glovebox; *n* equiv of Ag(CF_3SO_3) ($n = 2-5$) was dissolved in 15 mL of CH_2Cl_2 and the mixture vigorously stirred. A solution of compound **2** (200 mg) in 15 mL of CH_2Cl_2 was slowly added dropwise. After 0.5 h, the solution was filtered with a cannula under argon and rapidly evaporated to dryness. The product was dried under vacuum for several hours: 339 mg, 83% yield ($n = 5$). Anal. Calcd for **11**, $C_{34}H_{42}N_2O_{14}Fe_2S_4F_{12}$: C, 34.89; H, 3.62; N, 2.39. Found: C, 34.48; H, 3.76; N, 2.52.

Electrochemical Oxidation of 5: Synthesis of $[2(Me)_2][BF_4]_4$ (12). After a controlled-potential electrolysis at 0.8 V of a solution of **5** (75.4 mg in 10 mL of CH_3CN, Et_4NBF_4), the blue electrochemical mixture was immediately evaporated to dryness for 4 h. The product was extracted with several fractions of CH_2Cl_2 (15, 10, 5, and 3 mL). The solvent was evaporated, yielding a blue product. Anal. Calcd for **12**, $C_{32}H_{46}N_2O_2Fe_2B_4F_{16}$: C, 40.41; H, 4.88; N, 2.95. Found: C, 40.24; H, 4.78; N, 2.75.

Crystallographic Study of Compound (7). The data collection was performed at low temperature ($T = -93$ °C) on an I.P.D.S. STOE using graphite-monochromatized Mo Kα radiation and equipped with an Oxford Cryostream cooling device. The structure was solved by direct methods using SIR92[39] and subsequent Fourier maps. The refinement was performed by using the full-matrix least-squares technique with the CRYSTALS package.[40] All hydrogen atoms were found on difference Fourier maps, but they were included in the refinement process as fixed contributors with C−H = 0.96 Å and isotropic thermal parameters fixed 20% higher than those of their carbon atoms. Their positions were calculated after each refinement cycle. All non-hydrogen atoms were anisotropically refined. Full-matrix least-squares refinement was carried out by minimizing the function $\sum w(|F_o| - |F_c|)^2$, where F_o and F_c are the observed and calculated structure factors. Models reached convergence with R and R_w values mentioned in Table 1. The molecule was drawn using CAMERON.[41]

Acknowledgment. Dr. René Mathieu (Toulouse, France) is gratefully acknowledged for fruitful discussion. We gratefully acknowledge Dominique de Montauzon (Service d'Electrochimie du LCC, CNRS) for expert technical assistance and fruitful discussion. We thank Dr. Jean Claude Daran (Toulouse, France) for helpful discussions about the X-ray data, and Dr. Paul-Louis Fabre (Castres) is acknowledged for fruitful discussion. The suggestion provided by one of the reviewers, concerning the CV perturbation for the [Fe−Ag] compound, is also acknowledged.

Supporting Information Available: Complete crystal data, data collection, and refinement parameters (Table S1), fractional atomic coordinates and equivalent thermal parameters (Table S2), full list of interatomic distances (Table S3) and bond angles (Table S4), fractional atomic coordinates and isotropic thermal parameters for the H atoms (Table S5), anisotropic thermal parameters for the non-hydrogen atoms (Table S6) for **7**, 2D NMR data and selected spectra for **2** and **3a**, and expanded ^1H NMR (CD_3CN, 200 MHz) spectra at $\delta = 1.5-5.0$ ppm for **2**, **3a**, **4a**, and **5** (14 pages). Ordering information is given on any current masthead page. Observed and calculated structure factors have been deposited at the Cambridge Crystallographic Data Center. Copies of the data can be obtained, free of charge, on application to the Director, CCDC, 12 Union Road, Cambridge CB2 1EC, U.K.

IC970017R

---

(39) Altomare, A.; Cascarano, G.; Giacovazzo, G.; Guargliardi, A.; Burla, M. C.; Polidori, G.; Camalli, M. *SIR92*, a program for automatic solution of crystal structures by direct methods. *J. Appl. Crystallogr.* **1992**, *27*, 435.

(40) Watkin, D. J.; Prout, C. K.; Carruthers, R. J.; Betteridge, P. *CRYSTALS Issue 10*; Chemical Crystallography Laboratory, University of Oxford: Oxford, 1996.

(41) Watkin, D. J.; Prout, C. K.; Pearce, L. J. *CAMERON*; Chemical Crystallography Laboratory, University of Oxford: Oxford, U.K., 1996.